scientific reports

Check for updates

OPEN

OCTA changes of retinal microvessels and thickness in moyamoya disease

Xian-Zhe Qian[1,5], Cheng Chen[1,5], Hong-Liang Li[1,5], Lei Zhong[2], Hong Wei[1], Qian-Min Ge[1], Jin-Yu Hu[1], Qi Hong[1], Xiao-Yu Wang[1], Yan-Mei Zeng[1], Xu Chen[3], Yi-Xin Wang[4], Chong-Gang Pei[1]✉ & Yi Shao[2]✉

Moyamoya disease (MMD) is a structural abnormality of the cerebral vasculature characterized by cerebral ischemia, and is rare but its incidence is increasing. Digital subtraction angiography (DSA) of the brain is the primary means of diagnosing and evaluating this disease. But its high price and invasiveness limit its use as a monitoring tool for disease progression. As a non-invasive test for ophthalmic disorders, the optical coherence tomography angiography (OCTA) is widely used. In addition to ophthalmic diseases, OCTA has also been used in some neurological diseases. The aim of this study was to assess fundus changes in patients with MMD by OCTA and to investigate whether these changes could be a diagnostic and assessment marker for MMD. This study evaluated cerebral vessels, superficial macular capillary vessel density (SMC-VD) and macular retinal thickness (MRT) in subjects in the non-operated group (nGO), operated group (OG) and healthy controls (HC) using DSA, OCTA and other techniques. Analyses of variance (ANOVA) and Bonferroni post hoc analysis were used to calculate statistical differences between the three groups. Correlations between SMC-VD and MRT were assessed using Pearson correlation analysis. In addition, the ability of the SMC-VD and the MRT to distinguish MMD from HC was analyzed using receiver operating characteristic (ROC) curves. We found that the SMC-VD and MRT in the nOG group were significantly lower than those in the HC group and had not returned to normal levels at one month postoperatively. In the nOG, the SMC-VD and MRT were positively correlated in the Full region (6*6 mm) and in the Inner region (3*3 mm), and in many subregions they showed high ability to distinguish MMD from HC. The above findings indicate significant reduction in the SMC-VD and the MRT in patients with MMD even in the absence of ocular clinical manifestation. Most importantly, SMC-VD and MRT have a strong ability to distinguish between MMD patients and HC, suggesting that OCTA, a relatively inexpensive and non-invasive method, is useful in assessing cerebrovascular changes in MMD patients.

Keywords Moyamoya disease, Vessel density, Retinal thickness, OCTA, Diagnostic markers

A rare structural abnormality of the cerebral vasculature called moyamoya disease (MMD). It presents as the proximal intracranial segment of the internal carotid artery (ICA) is stenosed and the distal end is hyperplastic. The abundant collateral vessels at its distal end look like smoke[1–4]. Recent reports indicate that the average prevalence of MMD is 3.92/100,000 in China and about 10.5/100,000 in Japan, while the prevalence in the United States is only 1/11,000,000. However, in many regions globally, its prevalence has gradually increased in recent years[3,5–7]. The main clinical symptom of MMD is cerebral ischemia. Children often present with transient ischemic attack and adults with ischemic cerebral infarction. Complications such as seizures, headache, and cognitive dysfunction may also be associated with cerebral ischemia[2,3,8,9] and cerebral ischemic events have a high risk of recurrence[10]. In previous studies, a few cases of MMD were reported with ocular complications[11–14]. For example, Ashok et al. reported a young man who had central retinal artery occlusion (CRAO) and was diagnosed with MMD[15]. Alekya et al. reported a case of the patient with both CRAO and MMD, whose optical coherence tomography (OCT) results suggested a reduction in retinal thickness[16].

[1]Department of Ophthalmology, The First Affiliated Hospital, Jiangxi Medical College, Nanchang University, Nanchang 330006, Jiangxi, China. [2]Department of Ophthalmology, Shanghai General Hospital, Shanghai Jiao Tong University School of Medicine, National Clinical Research Center for Eye Diseases, Shanghai 200080, China. [3]Ophthalmology Centre of Maastricht University, 6200 MS Maastricht, Limburg Province, The Netherlands. [4]School of optometry and vision science, Cardiff University, Cardiff, Wales CF24 4HQ, UK. [5]Xian-Zhe Qian, Cheng Chen and Hong-Liang Li contributed equally to this work. ✉email: peichonggang11@163.com; freebee99@163.com

As a revolutionary imaging method, optical coherence tomography angiography (OCTA) can provide quantitative and morphological data on retinal microvascular changes in vivo[17]. A variety of measures such as blood flow[18], size of FAZ[19], vessel density and others[20] can be calculated using the OCTA technique. In addition, morphological data include vessel length, diameter and number of branches[21]. Currently, OCTA is widely used for the diagnosis and monitoring of ocular diseases which include glaucoma[22], age-related macular degeneration (AMD)[23], and diabetic retinopathy[24]. In the neurological system, OCTA is also considered to assist in monitoring the progression of Alzheimer's disease[25–27], multiple sclerosis[28–30], and other diseases.

To investigate whether microvascular and structural changes in the macula reflect the cerebrovascular status of patients with MMD, that is, whether OCTA can be an assistance in the diagnosis of MMD, we collected superficial macular capillary vessel density (SMC-VD) and macular retinal thickness (MRT) in MMD patients and healthy controls (HC). We also collected SMC-VD and MRT data from patients with MMD who had undergone revascularization in a bid to observe the impact of cerebral blood flow alterations on the retina.

Materials and methods

Subject recruitment

Thirty-two subjects with MMD who met the criteria were recruited by the diagnostic criteria for MMD proposed by the Japanese Committee for the Study of Spontaneous Occlusion of the Ring of Willis[31]. Sixteen of them did not be treated surgically and were the non-operated group (nOG). The other 16 were treated with revascularization (superficial temporal artery-middle cerebral artery anastomosis) and were the operated group (OG). Healthy controls (HC) were included in the study with 16 subjects who met the appropriate criteria. All subjects were assessed between 2018 and 2022 by specialists in the relevant disciplines in the First Affiliated Hospital of Nanchang University.

Subjects for inclusion in nOG and OG matched the following criteria: (1) patients with classic MMD diagnosed by Digital subtraction angiography (DSA) and other exams; (2) OG patients undergoing revascularization for one month. Exclusion from the study: (1) DSA results are atypical and/or cannot be confirmed in patients with MMD; (2) other diseases that can affect the vasculature of the brain or a history of brain surgery (e.g. atherosclerosis, congenital malformations of the cerebral vessels, cranio-cerebral tumours, old cerebral infarction, recent transient ischemic attack, cerebral haemorrhage, etc.) and moyamoya syndrome, which is caused by these diseases; (3) diseases or history of ocular surgery that can clearly affect the retina and its blood vessels (e.g. glaucoma, ocular tumours, age-related macular degeneration (AMD), etc.); (4) systemic diseases that can affect the retina and its blood vessels (e.g. diabetes, systemic lupus erythematosus (SLE), hypertension, etc.); (5) individuals who are unable to undergo DSA and/or OCT (e.g. with allergic reaction to contrast media).

16 HC were matched for age and gender to nOG and OG patients and met the following criteria: (1) absence of cerebrovascular diseases and history of cranio-cerebral surgery (e.g. MMD, atherosclerosis, congenital malformations of the cerebral vessels, cranio-cerebral tumours, old cerebral infarction, recent transient ischemic attack, cerebral haemorrhage, etc.) and moyamoya syndrome, which is caused by these diseases; (2) absence of diseases affecting the retina and its blood vessels or history of ocular surgery (e.g. AMD, glaucoma, ocular tumours, etc.); (3) without systemic diseases affecting the retina and its blood vessels (e.g. diabetes, SLE, hypertension, etc.); (4) acceptable for relevant investigations such as DSA and OCTA.

Clinical examinations

The following medical examinations were performed on all subjects: (1) routine blood and blood biochemical examinations, such as hemoglobin, triglycerides, total cholesterol, glucose, and electrolytes; (2) blood pressure examination; (3) visual acuity (VA); (4) DSA of the brain; (5) OCTA. (some clinical results that did not differ significantly are not shown in the article).

DSA

A DSA machine was applied to the subject to perform DSA of the brain. The patient was advised to take the appropriate position (supine position was chosen for this study). After proper disinfection and anaesthesia, a small incision is opened at the puncture site and a guide wire is inserted using a puncture needle, along which an arterial sheath is placed. The imaging modality (internal carotid arteriography, common carotid arteriography, etc.) is chosen according to the subject's actual condition. A pigtail tube is connected and 5–8 ml of contrast media is injected uniformly at the appropriate location. Frontal and lateral contrast examinations are performed after adjusting the contrast field under fluoroscopy and the results are recorded.

OCTA

We use the Carl Zeiss Meditec AngioPlex system for OCTA imaging. This SD-OCT system operates at an A-scan speed of 68,000 scans per second, a 840 nm light source centre and a 90 nm bandwidth. The system operates with an axial resolution of 5 μm, a 15 μm lateral resolution and a 2.0 mm A-scan depth parameter. Each eye recorded 6*6 mm and 3*3 mm 3D OCTA images. After scanning, each retina of 6*6 mm was divided into nine Early Treatment Diabetic Retinopathy Study (ETDRS) subzones, comprising three concentric circles (1.0 mm, 3.0 mm and 6.0 mm radii, respectively). The 3*3 mm retina was divided into 5 subzones consisting of two concentric circles (radii of 1.0 mm and 3.0 mm, respectively). The vascular density is the percentage of the vascular perfusion area over the measured area. Vessel density was calculated from 2D frontal images created of the superficial retinal layers with a threshold method. Assigned each pixel to perfusion (1) or background (0) by identifying the value of the image block. Results from the region of interest were scaled according to pixel size to calculate the vascular density from the macular centre to the edges of the 6*6 mm and 3*3 mm images. The SMC-VD in this study ranged from the inner limiting membrane (ILM) to the inner plexiform layer (IPL). The left and right eyes of all subjects were evaluated.

	HC	nOG	OG	ANOVA
N	16	16	16	N/A
Eyes (N)	32	32	32	N/A
Age (year)	44.00 ± 12.90	49.44 ± 6.13	49.38 ± 8.71	0.200
Sex, male %	25.00%	18.75%	56.25%	0.055
Disease duration(month)	N/A	14.75 ± 30.40	27.56 ± 19.90	0.169
Visual acuity (log MAR)	4.67 ± 0.16	4.72 ± 0.17	4.75 ± 0.15	0.144
Systolic blood pressure (mm Hg)	122.86 ± 3.98	121.00 ± 13.87	127.44 ± 18.16	0.384
Diastolic blood pressure (mm Hg)	82.81 ± 4.81	82.82 ± 10.83	84.31 ± 12.24	0.884

Table 1. Fundamental information on the HC, nOG and OG. ANOVA Showed the Statistical Differences Across Groups. Age, disease duration, visual Acuity and blood puressure were expressed as mean ± SD. *HC* healthy controls, *nOG* non-operated group, *OG* operated group, *SD* standard deviation.

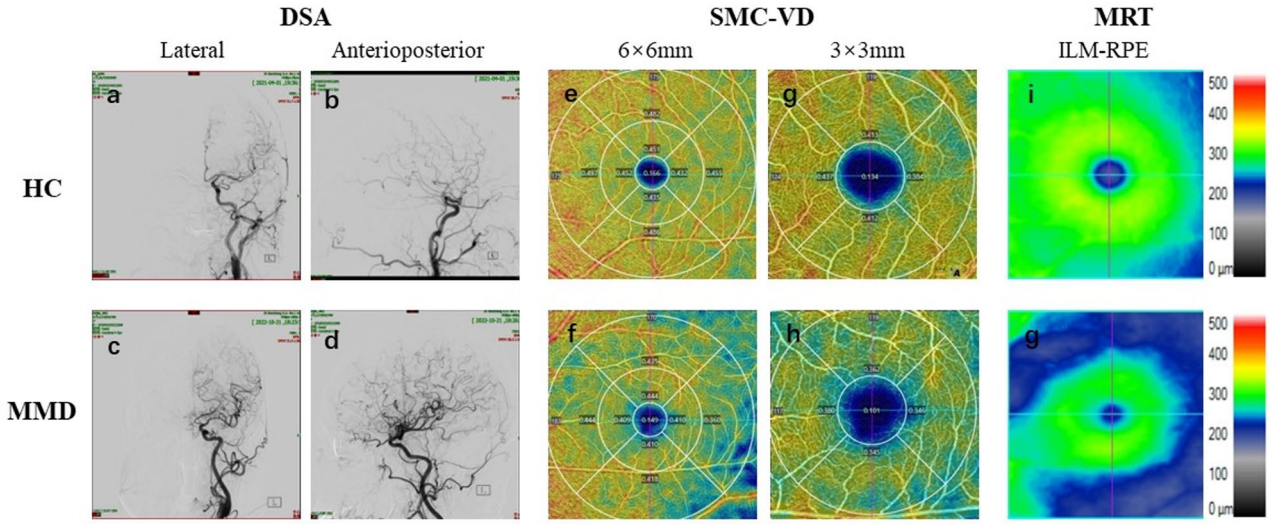

Fig. 1. Typical DSA, SMC-VD and MRT images of MMD patients and HC. **a** and **b** Anteroposterior view and lateral view of normal ICA angiraphy of HC. **c** and **d** internal carotid angiography in a patient with MMD shows abnormal smoke-like vessels. Suzuki is staged in III phases. **e** and **f** OCTA showed SMC-VD of 6*6 mm and 3*3 mm size in HC. **f** and **h** OCTA showing SMC-VD of 6*6 mm and 3*3 mm size in nOG. **i** MRT of HC. **g** MRT of nOG. Compared to HC, patients with MMD showed a significant reduction in SMC-VD and MRT. *DSA* digital subtraction angiography, *SMC-VD* superficial macular capillary vessel density, *MRT* macular retinal thickness, *MMD* moyamoya disease, *nOG* non-operated group, *HC* healthy controls, *OCTA* optical coherence tomography angiography.

Statistical analysis

Analysis of the results was performed with GraphPad Prism version 8 (La Jolla, California, USA) and SPSS version 22.0 (IBM, Armonk, NY, USA). Both ANOVA and Bonferroni Post Hoc Analysis were used for comparison between groups. G*power version 3.1 was used for efficacy analysis. Select one-way ANOVA, set parameters default values, and then select the VD of ON as an index. Calculating the effect value was 0.49 and the power was 0.77, which belonged to the large effect. Linear correlations between MRT and SMC-VD were performed for each group by applying person correlation analysis. For the analysis of differences between HC and MMD patients, subject work characteristic (ROC) curves were plotted.

Results

Fundamental information

As shown in Table 1, there were 16 subjects in the HC group, nOG and OG, respectively, in this study. It was analyzed for both eyes of each subject. The three groups of subjects did not differ in age ($p = 0.200$), gender ($p = 0.055$) and visual acuity (0.144) between the groups. Figure 1 illustrates typical DSA, SMC-VD and MRT images in MMD patients.

Analysis of the 6*6 mm SMC-VD

SMC-VD in the HC, nOG and the OG in the 6*6 mm region are shown in Table 2 and Fig. 2. The SMC-VD was markedly lower in the nOG than HC group in the IS ($p = 0.020$), OS ($p = 0.001$, cohen'd = 1.138), IN

Subregion	HC	nOG	OG	Bonferroni HC vs. nOG	Bonferroni HC vs. OG	ANOVA
Inner superior	0.455 ± 0.016	0.438 ± 0.030	0.448 ± 0.029	0.020	0.683	0.025
Outer superior	0.482 ± 0.012	0.464 ± 0.025	0.470 ± 0.024	0.001#	0.036#	0.002
Inner nasal	0.449 ± 0.015	0.421 ± 0.053	0.427 ± 0.047	0.016#	0.040#	0.020
Outer nasal	0.503 ± 0.015	0.469 ± 0.032	0.485 ± 0.014	< 0.001#	< 0.001#	< 0.001
Inner inferior	0.444 ± 0.017	0.440 ± 0.023	0.435 ± 0.040	1.000	0.674	0.475
Outer inferior	0.474 ± 0.018	0.459 ± 0.023	0.467 ± 0.028	0.028	0.765	0.032
Inner temporal	0.439 ± 0.027	0.433 ± 0.027	0.434 ± 0.038	1.000	1.000	0.654
Outer temporal	0.445 ± 0.028	0.429 ± 0.039	0.448 ± 0.030	0.168#	0.854#	0.047
Center	0.207 ± 0.060	0.194 ± 0.050	0.178 ± 0.060	1.000	0.130	0.128
Inner	0.446 ± 0.016	0.433 ± 0.025	0.435 ± 0.036	0.130	0.304	0.100
Outer	0.470 ± 0.014	0.456 ± 0.025	0.467 ± 0.020	0.020#	0.739#	0.017
Full	0.460 ± 0.013	0.446 ± 0.021	0.454 ± 0.023	0.019	0.663	0.023
FAZ	0.358 ± 0.140	0.311 ± 0.099	0.358 ± 0.054	0.586	1.000	0.334

Table 2. 6*6 mm SMC-VD (mean ± SD) in HC group, nOG and OG. Statistical differences between the nGO, OG and HC groups were calculated by ANOVA and Bonferroni post hoc analysis. *SMC-VD* superficial macular capillary vessel density, *SD* standard deviation, *HC* healthy controls, *nOG* non-operated group, *OG* operated group, *FAZ* fluorescein angiography zone. #Games-Howell Post Hoc Analysis display the Statistical Differences of the values with the heterogeneous variance.

($p = 0.016$), ON ($p < 0.001$, cohen'd = 1.521), OI ($p = 0.028$), Outer ($p = 0.022$) and Full ($p = 0.042$) regions. In regions II ($p = 1.000$), IT ($p = 1.000$), OT ($p = 0.168$), C ($p = 1.000$) and Inner (Inner, $p = 0.134$) decreases were not statistically significant (Table 2; Fig. 2a, c). In the OS ($p = 0.036$), IN ($p = 0.040$) and ON ($p < 0.001$, cohen'd = 1.800) subregions, the SMC-VD declined markedly in the OG. The alterations in the remaining subregions were not statistically significant (Table 2; Fig. 2b, d). The change in FAZ ($p = 0.334$) was also not statistically significant.

Analysis of the 3*3 mm SMC-VD

SMC-VD changes in the three groups in the 3*3 mm region are shown in Table 3 and Fig. 3. In comparison to the HC group, the SMC-VD was markedly decreased in the S ($p = 0.001$, cohen'd = 0.855), N ($p < 0.001$, cohen'd = 0.949), I ($p = 0.042$), T ($p = 0.001$, cohen'd = 1.038) and Inner ($p = 0.002$, cohen'd = 0.940) regions in nOG patients. Changes in SMC-VD in the C ($p = 0.084$) and Full ($p = 0.080$) regions were not statistically significant (Table 3; Fig. 3a, c). SMC-VD in the OG remained markedly lower than in the HC in the S ($p = 0.026$), N ($p = 0.002$, cohen'd = 1.009), I ($p = 0.039$), C ($p = 0.018$) and Inner ($p = 0.020$) regions. The SMC-VD was not statistically different from HC in T ($p = 0.686$) and Full ($p = 0.464$) subregions of the OG (Table 3; Fig. 3b, d). The change in FAZ ($p = 0.808$) was not statistically significant.

MRT

The MRT in the three groups are shown in Table 4 an Fig. 4. In all subregions except C ($p = 0.954$), MRT in the nOG was significantly thinner than in the HC group (IT, $p = 0.011$; $p < 0.001$ for all remaining regions; Table 4; Fig. 4a, c). Reductions in MRT remained in the IS ($p = 0.012$), IN ($p < 0.001$), ON ($p < 0.001$), Outer ($p = 0.008$) and Full ($p = 0.023$) regions in the OG compared with the HC group (Table 4; Fig. 4b, d).

Correlation analysis

In the nOG, SMC-VD in the Full region was positively correlated with the corresponding MRT value (Pearson $r = 0.590$, $p < 0.001$) (Fig. 5a), suggesting that a decrease in MRT was associated with a decrease in SMC-VD. The SMC-VD (3*3 mm) in the Inner region was correlated with the MRT in the corresponding subregion (Fig. 5b).

ROC curves

The ability of MRT to discriminate MMD is represented by the area under the curve (AUC) shown in Fig. 6a. The regions with AUC > 0.9 were ON (AUC = 0.989; $p < 0.001$), OI (AUC = 0.909; $p < 0.001$), OT (AUC = 0.912; $p < 0.001$), and Outer (AUC = 0.969; $p < 0.001$). The analysis of ROC curves for other regions is shown in Table 5. The diagnostic accuracy of SMC-VD for MMD is indicated by the AUC shown in Fig. 6b. The only region with AUC > 0.9 was ON (AUC = 0.907; $p < 0.001$). The analysis of ROC curves for other regions is shown in Table 6.

Discussion

We collected and compared SMC-VD and MRT in the nOG, OG and HC groups to investigate whether microvasculature and retinal thickness were altered in patients with MMD and to assess their diagnostic potential for MMD.

Most subregions of the nOG had lower SMC-VD than HC based on OCTA results (Tables 2, 3; Figs. 2, 3). This finding suggests that cerebral vascular disease in patients with MMD may affect superficial retinal capillary density. Several branches are given off by the ICA in the neck and skull, including the ophthalmic artery, which supplies blood to the eyes. The central retinal artery is derived from the ophthalmic artery and supplies blood to the inner five layers of the retina. Blood to the outer five layers of the retina is supplied primarily by the ciliary

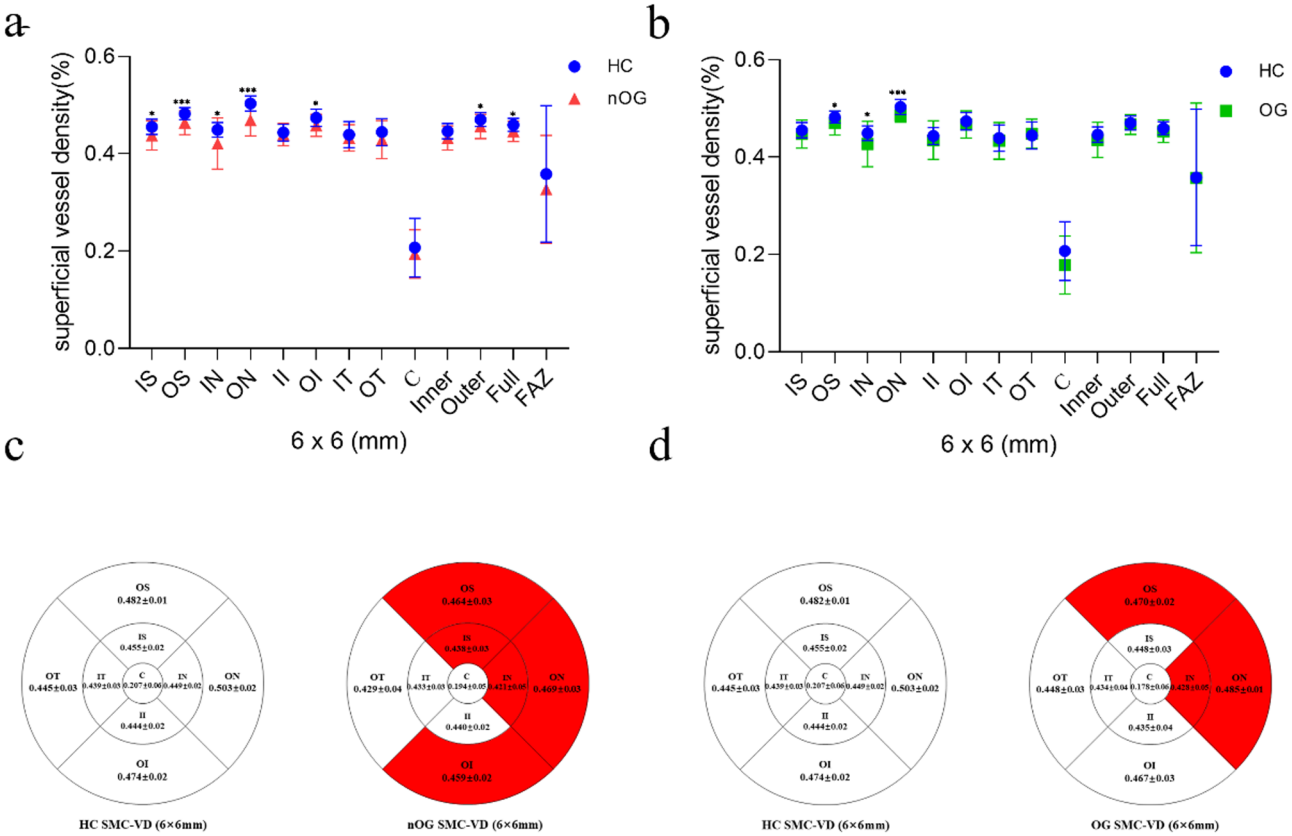

Fig. 2. SMC-VD analysis of 6*6 mm size in HC group, nOG and OG. **a** Statistical analysis of SMC-VD changes in the HC and nOG. IS ($p = 0.020$), OS ($p = 0.001$), IN($p = 0.016$), ON ($p < 0.001$), OI ($p = 0.028$), Outer ($p = 0.022$) and Full ($p = 0.042$) subregions showed a significant reduction in SMC-VD compared to HC. **b** Statistical analysis of SMC-VD changes in the HC and OG. The SMC-VD in the OS ($p = 0.036$), IN ($p = 0.040$) and ON ($p < 0.001$) subregions were significantly lower than that in the HC group. **c** Mean values of SMC-VD (6*6 mm) in each subregion of HC group and nOG. The red area indicates a significant decrease in SMC-VD in this region compared to HC. **d** Mean values of SMC-VD (6*6 mm) in each subregion of HC group and OG. The red area indicates a significant decrease in SMC-VD in this region compared to HC. $^{*}p < 0.05$; $^{**}p < 0.01$; $^{***}p < 0.001$. *SMC-VD* superficial macular capillary vessel density, *HC* healthy controls, *nOG* non-operated group, *OG* operated group, *IS* inner superior, *OS* outer superior, *IN* inner nasal, *ON* outer nasal, *OI* outer inferior, *FAZ* fluorescein angiography zone.

Subregion	HC	nOG	OG	Bonferroni HC vs. nOG	Bonferroni HC vs. OG	ANOVA
Superior	0.419 ± 0.022	0.397 ± 0.029	0.403 ± 0.021	0.001	0.026	0.001
Nasal	0.420 ± 0.016	0.396 ± 0.032	0.397 ± 0.028	< 0.001	0.002	< 0.001
Inferior	0.405 ± 0.017	0.388 ± 0.034	0.391 ± 0.025	0.042#	0.039#	0.030
Temporal	0.410 ± 0.013	0.388 ± 0.027	0.405 ± 0.028	0.001#	0.686#	0.001
Center	0.187 ± 0.051	0.158 ± 0.043	0.151 ± 0.060	0.084	0.018	0.015
Inner	0.412 ± 0.011	0.392 ± 0.028	0.400 ± 0.021	0.002#	0.020#	0.001
Full	0.379 ± 0.017	0.367 ± 0.027	0.371 ± 0.021	0.080	0.464	0.080
FAZ	0.360 ± 0.144	0.340 ± 0.099	0.356 ± 0.140	1.000	1.000	0.808

Table 3. 3*3 mm SMC-VD (mean ± SD) in HC group, nOG and OG. Statistical differences between the nGO, OG and HC groups were calculated by ANOVA and Bonferroni post hoc analysis. *SMC-VD* superficial macular capillary vessel density, *HC* healthy controls, *nOG* non-operated group, *OG* operated group, *FAZ* fluorescein angiography zone. #Games-Howell Post Hoc Analysis display the Statistical Differences of the values with the heterogeneous variance.

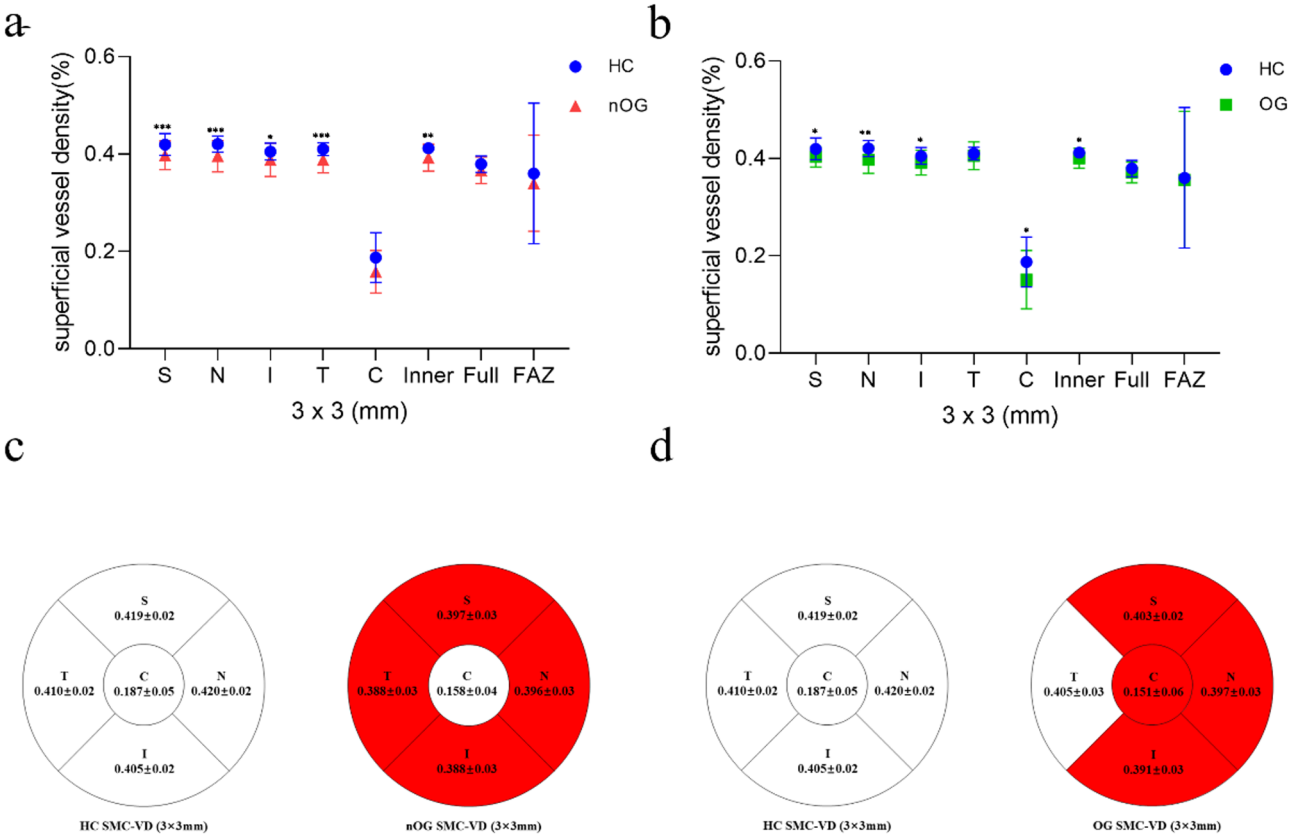

Fig. 3. SMC-VD analysis of 3*3 mm size in HC group, nOG and OG. **a** Statistical analysis of SMC-VD changes in the HC and nOG. S ($p = 0.001$), N ($p < 0.001$), I ($p = 0.042$), T ($p = 0.001$) and Inner ($p = 0.002$) subregions showed a significant reduction in SMC-VD compared to HC. **b** Statistical analysis of SMC-VD changes in the HC and OG. SMC-VD was significantly lower in the S ($p = 0.026$), N ($p = 0.002$), I ($p = 0.039$), C ($p = 0.018$) and Inner ($p = 0.020$) subregions than in the HC group. **c** Mean values of SMC-VD (3*3 mm) in each subregion of HC group and nOG. The red area indicates a significant decrease in SMC-VD in this region compared to HC. **d** Mean values of SMC-VD (3*3 mm) in each subregion of HC group and OG. The red area indicates a significant decrease in SMC-VD in this region compared to HC. $^{*}p < 0.05$; $^{**}p < 0.01$; $^{***}p < 0.001$. *SMC-VD* superficial macular capillary vessel density, *HC* healthy controls, *nOG* non-operated group, *OG* operated group, *S* superior, *N* nasal, *I* inferior, *T* temporal, *C* center, *FAZ* fluorescein angiography zone.

Subregion	HC	nOG	OG	Bonferroni HC vs. nOG	Bonferroni HC vs. OG	ANOVA
Inner superior	332.44 ± 14.70	312.94 ± 15.15	320.69 ± 17.94	< 0.001	0.012	< 0.001
Outer superior	298.59 ± 20.72	277.81 ± 16.06	287.91 ± 18.23	< 0.001	0.068	< 0.001
Inner nasal	330.06 ± 15.11	311.00 ± 15.35	307.19 ± 19.40	< 0.001	< 0.001	< 0.001
Outer nasal	317.25 ± 8.14	290.69 ± 11.24	274.28 ± 13.85	< 0.001	< 0.001	< 0.001
Inner inferior	323.50 ± 14.32	304.41 ± 22.22	321.88 ± 19.58	< 0.001	1.000	< 0.001
Outer inferior	279.19 ± 5.38	262.50 ± 13.37	282.00 ± 14.87	< 0.001#	0.578#	< 0.001
Inner temporal	316.50 ± 14.28	303.25 ± 14.96	315.84 ± 22.88	0.011	1.000	0.005
Outer temporal	275.69 ± 7.12	261.13 ± 9.17	295.34 ± 22.38	< 0.001#	< 0.001#	< 0.001
Center	238.75 ± 22.85	243.91 ± 21.78	241.78 ± 16.40	0.954	1.000	0.603
Inner	325.75 ± 12.83	308.03 ± 14.30	316.47 ± 18.74	< 0.001	0.056	< 0.001
Outer	292.75 ± 7.44	273.19 ± 11.27	285.00 ± 10.94	< 0.001	0.008	< 0.001
Full	301.28 ± 9.49	285.31 ± 10.06	294.19 ± 11.50	< 0.001	0.023	< 0.001

Table 4. MRT (mean ± SD) in HC group, nOG and OG. Statistical differences between the nGO, OG and HC groups were calculated by ANOVA and Bonferroni post hoc analysis. *MRT* macular retinal thickness, *HC* healthy controls, *nOG* non-operated group, *OG* operated group, *FAZ* fluorescein angiography zone. #Games-Howell Post Hoc Analysis display the Statistical Differences of the values with the heterogeneous variance.

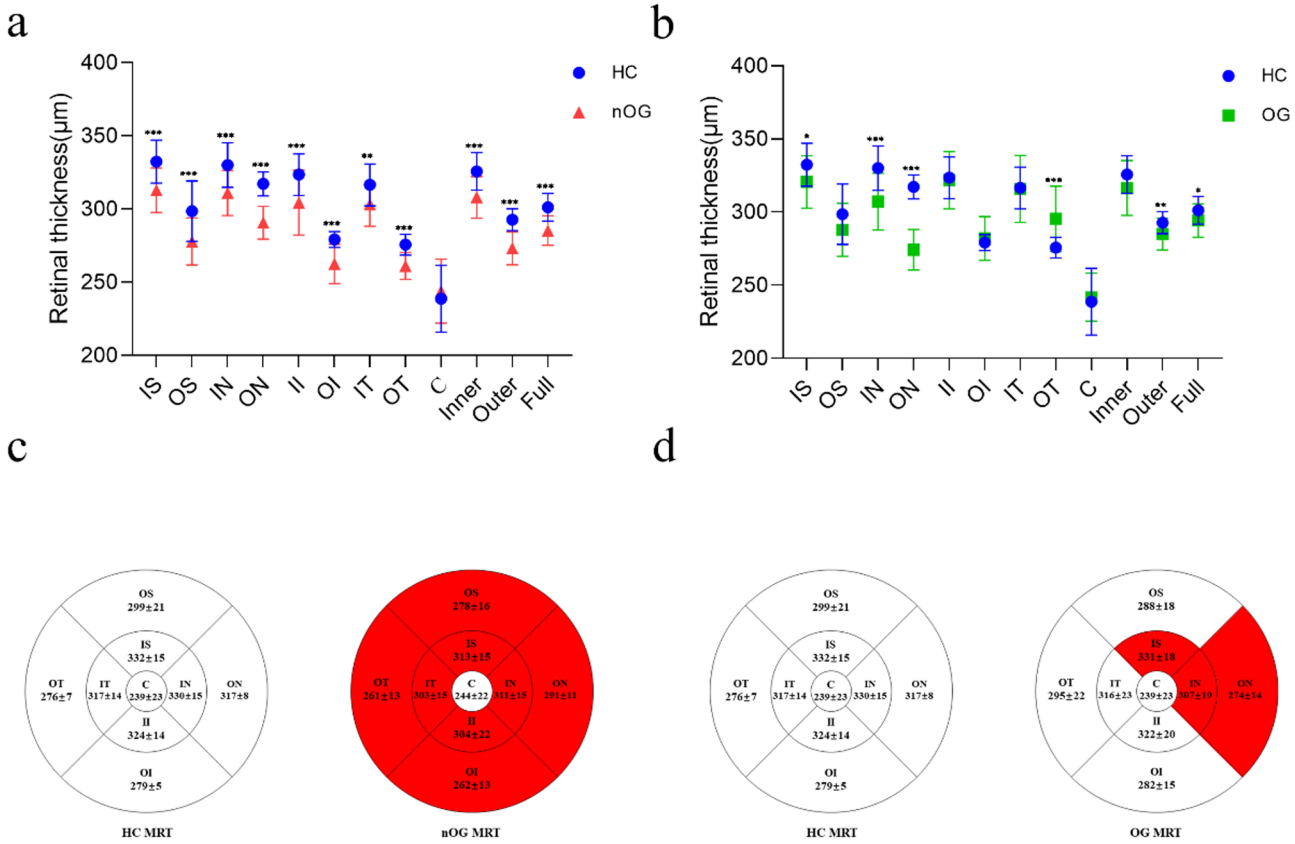

Fig. 4. MRT analysis of HC group, nOG and OG. **a** Statistical analysis of MRT changes in the HC and nOG. All subregions except subregion C displayed a marked reduction in MRT compared to HC (IT, $p = 0.011$; $p < 0.001$ for all remaining regions). **b** Statistical analysis of MRT changes in the HC and OG. The MRT was markedly thinner in the IS ($p = 0.012$), IN ($p < 0.001$), ON ($p < 0.001$), OT ($p < 0.001$), outer ($p = 0.008$) and full ($p = 0.023$) regions in comparison to the HC group. **c** Mean values of MRT in each subregion of HC group and nOG. The red area indicates a significant decrease in MRT in this region compared to HC. **d** Mean values of MRT in each subregion of HC group and OG. The red area indicates a significant decrease in MRT in this region compared to HC $^{*}p < 0.05$; $^{**}p < 0.01$; $^{***}p < 0.001$. *MRT* macular retinal thickness, *HC* healthy controls, *nOG* non-operated group, *OG* operated group, *IS* inner superior, *OS* outer superior, *IN* inner nasal, *ON* outer nasal, *II* inner inferior, *OI* outer inferior, *IT* inner temporal, *OT* outer temporal, *C* center, *FAZ* fluorescein angiography zone.

artery system emanating from the ophthalmic artery[32–36]. Blood from the central retinal artery supplies the retinal nerve fiber layer, ganglion cell layer and inner plexiform layer through the superficial capillary plexus (SCP), and continues to extend to become the deep capillary plexus (DCP) in the inner nuclear layer. The radial peripapillary capillary plexus (RPCP) is in the nerve fibre layer (NFL)that runs parallel to the axons of the nerve fibres[32,37–40]. The capillaries of the SMC-VD we measured in this study are part of the temporal branch of the SCP (Fig. 7). The temporal retinal arteries arch around the macula, forming the superior macular arteriole and the arteriola macularis inferior[34,35] (Fig. 7). Stenosis of the ICA is a feature of MMD, and in these cases the blood supply to the branches of the ICA will be reduced. Previous studies have also suggested that retinal ischemia is associated with severe stenosis of the ICA[41,42]. Therefore, we suggested that the narrowing of ICA led to the reduction of SMC-VD.

These changes suggest questions about their role in structural and functional variations in the retina. In the present study, MRT of patients in the nOG was significantly thinner than that of healthy subjects in all subregions but C (Table 4; Fig. 4), yet these subjects did not show significant visual impairment. Blockage of the central retinal artery and its branches can often be observed as retinal edema[33,34,39,43,44]. Due to ischemia and hypoxia, the retinal cells become edematous, and if ischemia is prolonged the inner retinal cells gradually become necrotic, leading to reduced retinal thickness[34,39]. The MMD subjects we included in our study all had long disease duration (Table 1). Therefore, we interpret their MRT reduction as an alteration caused by prolonged ischemia and hypoxia. That means the reduction of MRT is associated with the reduction of SMC-VD. And a correlation was found in nOG between MRT and SMC-VT in the Full region at 6*6 mm (Fig. 5a) and in the Inner region at 3*3 mm (Fig. 5b). This evidence indicates a close association between reduced MRT and reduced SMC-VD in patients with MMD.

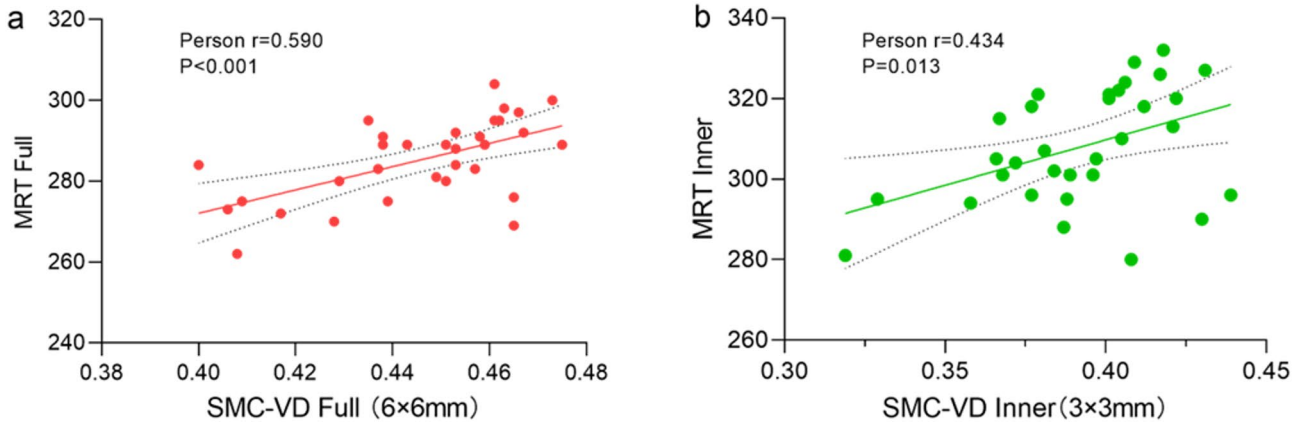

Fig. 5. The correlation between MRT and SMC-VD. **a** Full SMC-VD of 6*6 mm sizes in MMD patients (nOG) was positively correlated with the corresponding MRT (Person $r = 0.590$, $p < 0.001$). **b** In patients with MMD (nOG), a correlation was found between the full SMC-VD of 3 × 3 mm and the corresponding MRT values (Person $r = 0.434$, $p = 0.013$). *MRT* macular retinal thickness, *SMC-VD* superficial macular capillary vessel density, *MMD* moyamoya disease, *HC* healthy controls, *nOG* non-operated group.

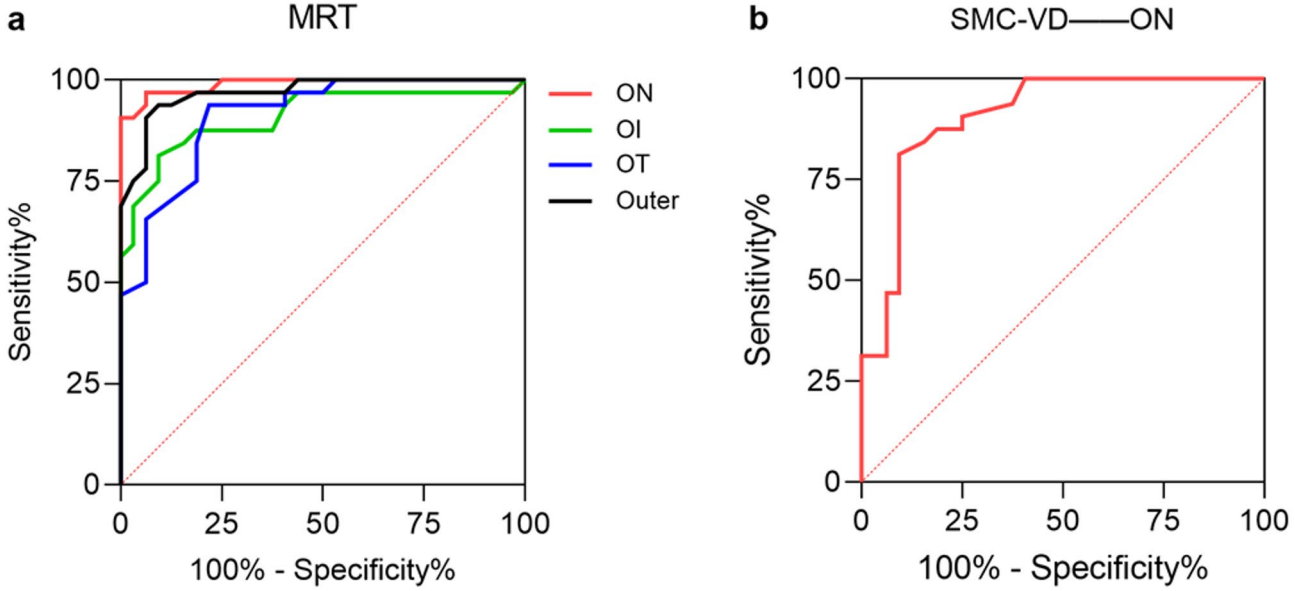

Fig. 6. ROC curves of MRT and SMC-VD. **a** The AUC suggests the accuracy of MRT for the diagnosis of MMD. The AUC in the ON (AUC = 0.989), OI (AUC = 0.909), OT (AUC = 0.912) and Outer (AUC = 0.969) subregions was greater than 0.9. **b** The AUC suggests accuracy of SMC-VD for MMD diagnosis. The AUC in the ON (AUC = 0.907) subregion was greater than 0.9. *ROC* receiver operating characteristic, *MRT* macular retinal thickness, *SMC-VD* superficial macular capillary vessel density, *AUC* area under ROC curve, *MMD* moyamoya disease, *ON* outer nasal, *OI* outer inferior, *OT* outer temporal.

To further investigate this link in patients with MMD we evaluated structural and microvascular variations in the retinas of MMD subjects one month after revascularization. The results indicated that in this group (OG) the SMC-VD remained significantly lower than HC in OS, IN, ON, S, I and Inner regions (Tables 2, 3; Fig. 2b, d, 3b, d). The MRT did not return to normal in the IS, IN, ON, Outer, and Full regions compared to HC (Table 4; Fig. 4b, d). We speculate that the above results may be due to the occurrence of ischemia-reperfusion injury. Ischemia-reperfusion injury mainly refers to tissue damage caused by the restoration of blood supply after ischemia or/and hypoxia[45,46]. This can manifest as endothelial damage, increased permeability and leukocyte obstruction in microvessels, especially small arteries and capillaries[47,48]. A recent case report also showed that a patient with MMD who underwent left superficial temporal artery-middle cerebral artery anastomosis for one month had a significantly reduced superficial retinal vessels of the left eye which did not return to normal until nine months postoperatively. This vascular complex, however, did not show any significant abnormality before surgery[49]. On the other hand, this suggests that even though vascular recanalization is immediately and

MRT	AUC	SE	95% CI	*P* value
Inner superior	0.815	0.052	0.714 to 0.917	<0.001
Outer superior	0.839	0.050	0.741 to 0.937	<0.001
Inner nasal	0.796	0.054	0.690 to 0.902	<0.001
Outer nasal	0.989	0.009	0.972 to 1.000	<0.001
Inner inferior	0.804	0.056	0.695 to 0.913	<0.001
Outer inferior	0.909	0.039	0.832 to 0.986	<0.001
Inner temporal	0.735	0.062	0.614 to 0.856	0.001
Outer temporal	0.912	0.034	0.845 to 0.979	<0.001
Center	0.574	0.072	0.432 to 0.716	0.308
Inner	0.818	0.051	0.718 to 0.919	<0.001
Outer	0.969	0.018	0.933 to 1.000	<0.001
Full	0.872	0.042	0.790 to 0.955	<0.001

Table 5. ROC curve analysis of MRT. AUC values, SE, 95% CI and P values for each subregion. *ROC* receiver operating characteristic, *MRT* macular retinal thickness, *AUC* area under ROC curve, *SE* standard errors, *95% CI* 95% confidence intervals.

SMC-VD(6*6 mm)	AUC	SE	95% CI	*P* value
Inner superior	0.672	0.067	0.540 to 0.804	0.018
Outer superior	0.731	0.062	0.609 to 0.852	0.002
Inner nasal	0.648	0.069	0.513 to 0.784	0.041
Outer nasal	0.907	0.038	0.832 to 0.981	<0.001
Inner inferior	0.560	0.075	0.413 to 0.706	0.413
Outer inferior	0.698	0.067	0.567 to 0.829	0.007
Inner temporal	0.598	0.073	0.454 to 0.742	0.177
Outer temporal	0.607	0.072	0.466 to 0.748	0.142
Center	0.600	0.072	0.459 to 0.741	0.171
Inner	0.648	0.069	0.513 to 0.783	0.042
Outer	0.651	0.069	0.516 to 0.786	0.038
Full	0.673	0.067	0.543 to 0.804	0.017

Table 6. ROC curve analysis of SMC-VD(6*6 mm). AUC values, SE, 95% CI and P-values for each subregion. *ROC* receiver operating characteristic, *SMC-VD* superficial macular capillary vessel density, *AUC* area under ROC curve, *SE* standard errors, *95% CI* 95% confidence intervals.

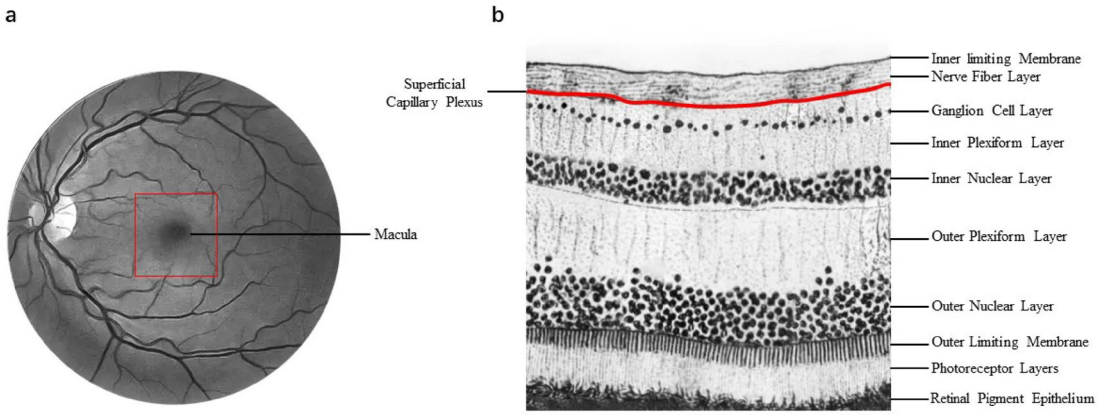

Fig. 7. Anatomical localization of retinal vessels and anatomical stratification of the retina. **a** The area circled by the red square is the approximate location of the macula as described in the study. **b** The SMC-VD we focused on in the study was mainly from superficial capillary plexus. *SMC-VD* superficial macular capillary vessel density.

significantly effective from DSA images, it may take several months or even longer for the actual blood vessels to fully recover. This phenomenon is commonly referred to as no-reflow phenomenon and is commonly seen in the coronary arteries but also in the cerebrovascular vessels. In this paper, we studied the retinal microvascular changes in patients after revascularization surgery for 1 month, when the retinal microvessels were likely to be in the stage of no-reflow, which may be related to the fact that capillary-related cells (such as endothelial cells, neutrophils, pericytes, etc.) have not yet returned to normal function. It has also been shown that patients with MMD have cerebral hyperperfusion and a range of complications after revascularization treatment[50,51]. On this basis, it seems feasible that in the present study small arteries and capillaries in the macula may have suffered reperfusion injury in addition to ischemia. In future studies we may need more specialized neurologists to evaluate the results of cerebral revascularization, rather than assuming that the cerebral vessels are back to normal just by the results of DSA.

Although the cerebral vascular system has a complex structure, Goto et al. suggested that retinal vasculopathy may in part reflect cerebral microvascular lesions[52–54]. In embryology, the retina was considered to be the central nervous system's extension with a common origin in the embryonic neural tube. The anterior part of the neural tube differentiates into brain tissue and forms a pair of optic vesicles which develop into the right and left retinas[35,55,56]. Moreover, anatomically, blood of the retina, the anterior two-thirds of the telencephalon, and part of the mesencephalon are supplied by the ICA[35,36,57] and alterations in the retinal arteries are related to vascular disease in the brain[58,59]. Strokes have been linked to retinal vessel changes even since the early studies using fundus photography[60,61] and changes in cognitive abilities[62,63]. We therefore hypothesized that OCTA measurement of retinal vascular structure and perfusion may also reflect in part the cerebral blood flow in patients with MMD. We evaluated the diagnostic accuracy of MRT and SMC-VD for MMD using ROC curves. The results showed high AUC values for MRT in all sub-regions except for region C. The AUC values of ON, OI, OT and Outer were all over 0.9, and approaching this value (at 0.87) in the Full region (Table 5; Fig. 6a). It is suggested that MRT has strong potential to discriminate between MMD and HC. This makes it possible for MRT to be used as a new tool for screening or adjuvant diagnosis of MMD. However, for SMC-VD only ON had an AUC greater than 0.9, values of the remaining subregions being mostly in the range of 0.6–0.7 (Table 6; Fig. 6b). The diagnostic accuracy of SMC-VD for MMD was therefore inferior to that of MRT. In our analysis, this may reflect the fact that vascular lesions in MMD affect not only the superficial retinal vessels, but also the deeper vascular layers, such as those of the choroid.

However, OCTA has the advantages of high resolution, non-invasiveness, no need for contrast agent, and real-time observation of vascular dynamics, it still has its limitations compared with DSA, which has mature technology, such as the limited penetration of OCTA and the inability to develop deep blood vessels; the range of a single imaging is small, and a wide range of blood vessels cannot be observed; It is impossible to accurately locate the lesion site of the diseased blood vessel and provide precise help for clinical surgical treatment. The limitations of our study need to be considered. For example, our sample size was so small that it limited the accuracy of the study. The relative age of the participants selected for this study was on the older side in order to collect as large a sample size as possible, but this may have more limitations. In the study, we only focused on the capillaries in the superficial layers of the retina. Other vessels of the retina, such as the DCP and choroidal capillaries, may also altered. In addition, Although the ophthalmic artery is affected by insufficient blood supply, we consider the ophthalmic artery to be hardly used as collateral access to compensate for the lack of blood supply to the internal carotid artery. And, we should assess the correspondence between cerebral and retinal vascular alterations by long-term, relatively frequent DSA and OCTA in future studies.

Conclusion

In summary, we conclude that patients with MMD still have significant SMC-VD and MRT reduction even in the absence of ocular clinical manifestations. And MRT reduction is closely associated with SMC-VD reduction. These reductions are not immediately restored with the re-establishment of cerebral blood flow. This may be related to ischemia-reperfusion damage to the retinal arteries. Importantly, the SMC-VD and MRT have a strong ability to distinguish MMD from HC, suggesting that alterations in retinal microvasculature and structure may be a cheaper non-invasive marker for assessing vascular changes in the brain in patients with MMD. The OCTA may serve as a more convenient way to monitor changes in MMD.

Data availability

The datasets used and/or analyzed during the present study are available from the corresponding author on reasonable request.

Received: 24 October 2024; Accepted: 23 June 2025
Published online: 01 July 2025

References

1. Suzuki, J. & Takaku, A. Cerebrovascular Moyamoya disease. Disease showing abnormal net-like vessels in base of brain. *Arch. Neurol.* **20**, 288–299 (1969).
2. Scott, R. M. & Smith, E. R. Moyamoya disease and Moyamoya syndrome. *N Engl. J. Med.* **360**, 1226–1237 (2009).
3. Shang, S. et al. Progress in Moyamoya disease. *Neurosurg. Rev.* **43**, 371–382 (2020).
4. Kiyoshi, T. S., Sato, M. & Disease *Cerebrovascular diseases in children* 227–243 (Springer, 1992).
5. Goto, Y. & Yonekawa, Y. Worldwide distribution of Moyamoya disease. *Neurol. Med. Chir. (Tokyo)*. **32**, 883–886 (1992).
6. Kuroda, S. & Houkin, K. Moyamoya disease: current concepts and future perspectives. *Lancet Neurol.* **7**, 1056–1066 (2008).
7. Hishikawa, T., Sugiu, K. & Date, I. Moyamoya disease: a review of clinical research. *Acta Med. Okayama*. **70**, 229–236 (2016).
8. Kim, S. K. et al. Pediatric Moyamoya disease: an analysis of 410 consecutive cases. *Ann. Neurol.* **68**, 92–101 (2010).

9. Kazumata, K. et al. Chronic ischemia alters brain microstructural integrity and cognitive performance in adult Moyamoya disease. *Stroke* **46**, 354–360 (2015).
10. Chiu, D., Shedden, P., Bratina, P. & Grotta, J. C. Clinical features of Moyamoya disease in the united States. *Stroke* **29**, 1347–1351 (1998).
11. Slamovits, T. L., Klingele, T. G., Burde, R. M. & Gado, M. H. Moyamoya disease with central retinal vein occlusion. Case report. *J. Clin. Neuroophthalmol.* **1**, 123–127 (1981).
12. Chace, R. & Hedges III, T. R. Retinal artery occlusion due to Moyamoya disease. *J. Clin. Neuroophthalmol.* **4**, 31–34 (1984).
13. Ushimura, S., Mochizuki, K., Ohashi, M., Ito, S. & Hosokawa, H. Sudden blindness in the fourth month of pregnancy led to diagnosis of Moyamoya disease. *Ophthalmologica* **207**, 169–173 (1993).
14. Albrecht, P. et al. Retinal pathology in idiopathic Moyamoya angiopathy detected by optical coherence tomography. *Neurology* **85**, 521–527 (2015).
15. Kumar, M. A. & Ganesh, B. A. CRAO in Moyamoya disease. *J. Clin. Diagn. Res.* **7**, 545–547 (2013).
16. Rajanala, A. P., Le, H. T. & Gill, M. K. Central retinal artery occlusion as initial presentation of Moyamoya disease in a middle-aged woman. *Am. J. Ophthalmol. Case Rep.* **18**, 100705 (2020).
17. Campbell, J. P. et al. Detailed vascular anatomy of the human retina by Projection-Resolved optical coherence tomography angiography. *Sci. Rep.* **7**, 42201 (2017).
18. Wang, R. K., Zhang, Q., Li, Y. & Song, S. Optical coherence tomography angiography-based capillary velocimetry. *J. Biomed. Opt.* **22**, 66008 (2017).
19. Choi, J. et al. Quantitative optical coherence tomography angiography of macular vascular structure and foveal avascular zone in glaucoma. *PLoS One*. **12**, e0184948 (2017).
20. Akil, H., Falavarjani, K. G., Sadda, S. R. & Sadun, A. A. Optical coherence tomography angiography of the optic disc; an overview. *J. Ophthalmic Vis. Res.* **12**, 98–105 (2017).
21. Wylęgała, A., Wylęgała, F. & Wylęgała, E. Aflibercept treatment leads to vascular abnormalization of the choroidal neovascularization. *J. Healthc. Eng.* **2018**, 8595278 (2018).
22. Scripsema, N. K. et al. Optical coherence tomography angiography analysis of perfused peripapillary capillaries in primary open-angle glaucoma and normal-tension glaucoma. *Investig. Ophthalmol. Vis. Sci.* **57**, Oct611–oct620 (2016).
23. Roisman, L., Goldhardt, R., Angiography, O. C. T. & An upcoming non-invasive tool for diagnosis of age-related macular degeneration. *Curr. Ophthalmol. Rep.* **5**, 136–140 (2017).
24. Schaal, K. B. et al. Vascular abnormalities in diabetic retinopathy assessed with swept-source optical coherence tomography angiography widefield imaging. *Retina* **39**, 79–87 (2019).
25. Ferrari, L. et al. Optical coherence tomography reveals retinal neuroaxonal thinning in frontotemporal dementia as in alzheimer's disease. *J. Alzheimers Dis.* **56**, 1101–1107 (2017).
26. Santos, C. Y. et al. [P4–058]: Retinal nerve fiber layer and ganglion cell layer volume changes in preclinical Alzheimer's disease over 27 months. *Alzheimer's Dement.* **13** (2017).
27. Santos, C. Y. et al. Change in retinal structural anatomy during the preclinical stage of alzheimer's disease. *Alzheimers Dement. (Amst).* **10**, 196–209 (2018).
28. Behbehani, R. et al. Optical coherence tomography segmentation analysis in relapsing remitting versus progressive multiple sclerosis. *PLoS One*. **12**, e0172120 (2017).
29. Feucht, N. et al. Optical coherence tomography angiography indicates associations of the retinal vascular network and disease activity in multiple sclerosis. *Mult Scler.* **25**, 224–234 (2019).
30. Oertel, F. C., Zimmermann, H. G., Brandt, A. U. & Paul, F. Novel uses of retinal imaging with optical coherence tomography in multiple sclerosis. *Expert Rev. Neurother.* **19**, 31–43 (2019).
31. Fujimura, M. & Tominaga, T. Diagnosis of Moyamoya disease: international standard and regional differences. *Neurol. Med. Chir. (Tokyo)*. **55**, 189–193 (2015).
32. Stone, J., van Driel, D., Valter, K., Rees, S. & Provis, J. The locations of mitochondria in mammalian photoreceptors: relation to retinal vasculature. *Brain Res.* **1189**, 58–69 (2008).
33. Mac Grory, B. et al. Management of central retinal artery occlusion: a scientific statement from the American heart association. *Stroke* **52**, e282–e294 (2021).
34. K.B.F.D.S.W.F.M.L.A. & Yannuzzi The Retinal Atlas, second deition, (2017).
35. Shitian, Z. D., Zhong, Z., Wang, Z. & Liu, Jianhua, Y. Clinical Anatomy of Ophthalmology, second edition, (2020).
36. Zuguo, N. W., Liu, X. & Sun Luosheng Tang 眼科学基础, 人民卫生出版社, (2018).
37. Henkind, P. Radial peripapillary capillaries of the retina. I. Anatomy: human and comparative. *Br. J. Ophthalmol.* **51**, 115–123 (1967).
38. Provis, J. M. Development of the primate retinal vasculature. *Prog. Retin Eye Res.* **20**, 799–821 (2001).
39. Antonia, T. W. G., Joussen, M., Kirchhof, B. & Ryan, S. J. Retinal Vascular Disease, (2011).
40. David, P. R. R.Chow, OCT Angiography, (2018).
41. Mizener, J. B., Podhajsky, P. & Hayreh, S. S. Ocular ischemic syndrome. *Ophthalmology* **104**, 859–864 (1997).
42. Babikian, V. et al. Retinal ischemia and embolism. Etiologies and outcomes based on a prospective study. *Cerebrovasc. Dis.* **12**, 108–113 (2001).
43. Hayreh, S. S. Acute retinal arterial occlusive disorders. *Prog. Retin Eye Res.* **30**, 359–394 (2011).
44. Ochakovski, G. A. et al. Retinal oedema in central retinal artery occlusion develops as a function of time. *Acta Ophthalmol.* **98**, e680–e684 (2020).
45. Jianzhi, R. Q., Wang, L., Wu, L., Sun, W. & Li Zhisheng Jiang 病理生理学, 人民卫生出版社, (2018).
46. Y.G. Xianzhong Xiao, 病理生理学, 高等教育出版社, (2018).
47. Carden, D. L. & Granger, D. N. Pathophysiology of ischaemia–reperfusion injury. *J. Pathol.* **190**, 255–266 (2000).
48. Eltzschig, H. K. & Eckle, T. Ischemia and reperfusion—from mechanism to translation. *Nat. Med.* **17**, 1391–1401 (2011).
49. Lo, K. J., Wang, A. G. & Cheng, H. C. Retinal vasculature changes after bypass surgery for moyamoya disease. *Ophthalmology* **128**, 120 (2021).
50. Kuroda, S., Kamiyama, H., Abe, H., Asaoka, K. & Mitsumori, K. Temporary neurological deterioration caused by hyperperfusion after extracranial-intracranial bypass–case report and study of cerebral hemodynamics. *Neurol. Med. Chir. (Tokyo)*. **34**, 15–19 (1994).
51. Fujimura, M., Kaneta, T., Mugikura, S., Shimizu, H. & Tominaga, T. Temporary neurologic deterioration due to cerebral hyperperfusion after superficial temporal artery-middle cerebral artery anastomosis in patients with adult-onset Moyamoya disease. *Surg. Neurol.* **67**, 273–282 (2007).
52. Goto, I., Katsuki, S., Ikui, H., Kimoto, K. & Mimatsu, T. Pathological studies on the intracerebral and retinal arteries in cerebrovascular and noncerebrovascular diseases. *Stroke* **6**, 263–269 (1975).
53. Patton, N. et al. Retinal vascular image analysis as a potential screening tool for cerebrovascular disease: a rationale based on homology between cerebral and retinal microvasculatures. *J. Anat.* **206**, 319–348 (2005).
54. Moss, H. E. Retinal vascular changes are a marker for cerebral vascular diseases. *Curr. Neurol. Neurosci. Rep.* **15**, 40 (2015).
55. Stenkamp, D. L. Development of the vertebrate eye and retina. *Prog. Mol. Biol. Transl. Sci.* **134**, 397–414 (2015).
56. Miesfeld, J. B. & Brown, N. L. Eye organogenesis: a hierarchical view of ocular development. *Curr. Top. Dev. Biol.* **132**, 351–393 (2019).

57. Rim, T. H., Teo, A. W. J., Yang, H. H. S., Cheung, C. Y. & Wong, T. Y. Retinal vascular signs and cerebrovascular diseases. *J. Neuroophthalmol.* **40**, 44–59 (2020).
58. Hughes, A. D. et al. Association of retinopathy and retinal microvascular abnormalities with stroke and cerebrovascular disease. *Stroke* **47**, 2862–2864 (2016).
59. Nelis, P. et al. OCT-angiography reveals reduced vessel density in the deep retinal plexus of CADASIL patients. *Sci. Rep.* **8**, 8148 (2018).
60. Lindley, R. I. et al. Retinal microvasculature in acute lacunar stroke: a cross-sectional study. *Lancet Neurol.* **8**, 628–634 (2009).
61. Kawasaki, R. et al. Fractal dimension of the retinal vasculature and risk of stroke: a nested case-control study. *Neurology* **76**, 1766–1767 (2011).
62. Patton, N. et al. The association between retinal vascular network geometry and cognitive ability in an elderly population. *Investig. Ophthalmol. Vis. Sci.* **48**, 1995–2000 (2007).
63. Ding, J. et al. Association of retinal arteriolar dilatation with lower verbal memory: the Edinburgh type 2 diabetes study. *Diabetologia* **54**, 1653–1662 (2011).

Acknowledgements
Not applicable.

Author contributions
HL. Li., C. Chen. and XZ. Qian wrote the main manuscript text and prepared Tables 1, 2 and 3. L. Zhong., H. Wei and QM. G. prepared Tables 4, 5 and 6 and Figs. 1, 2 and 3. JY. Hu and XY. Wang prepared Figs. 4 and 5. Q. Hong and YM. Zeng prepared Figs. 6 and 7. All authors reviewed the manuscript. Administrative support, Conception and design: Y. Shao and CG. Pei.

Funding
Supported by National Natural Science Foundation of China (No.82160195,82460203); Jiangxi Double-Thousand Plan High-Level Talent Project of Science and Technology Innovation(No.jxsq2023201036); Key R & D Program of Jiangxi Province (20223BBH80014); Science and Technology Project of Jiangxi Province Health Commission of Traditional Chinese Medicine (No. 2022B258); Science and Technology Project of Jiangxi Health Commission (No. 202210017).

Declarations

Competing interests
The authors declare no competing interests.

Ethical statement
Every aspect of the work is under the responsibility of the author, including the investigation and resolution of any questions of accuracy or integrity. A Medical Ethics Committee of Nanchang University First Affiliated Hospital (cdyfy2021039) approved the study based on the Declaration of Helsinki (revised 2013). All subjects voluntarily undertook to sign an informed consent form after understanding the potential risks, objectives and methods.

Additional information
Correspondence and requests for materials should be addressed to C.-G.P. or Y.S.